International Journal of Thermophysics, Vol. 6, No. 4, 1985

Experimental Determination of the Thermal Conductivity of Molten Pure Salts and Salt Mixtures

R. Tufeu,[1] J. P. Petitet,[1] L. Denielou,[1] and B. Le Neindre[1]

Received May 8, 1985

The thermal conductivity of some molten salts was measured at atmospheric pressure, using the coaxial cylinder method. The pure compounds $NaCO_3$, KNO_3, and $NaNO_2$, the equimolar mixture $NaNO_3$–KNO_3, and HITEC, which is a three-component mixture, $NaNO_3$–$NaNO_2$–KNO_3 (0.07–0.40–0.53 in weight), were investigated. For mixtures, it was found that the experimental thermal conductivity coefficients are in agreement with calculated values using a simple linear mixing law. The thermal diffusivity was calculated and compared with experimental data.

KEY WORDS: coaxial cylinder method; mixing rule; mixtures; molten salts; thermal conductivity; thermal diffusivity.

1. INTRODUCTION

The industrial applications of molten salts are increasing every year. They have unusual solvent properties which have led to their use in electrochemistry and metallurgical electrolysis. They have good hear transfer properties and have been considered to be used as transfer fluids in breeder reactors or fusion reactors, providing an increase in thermal efficiency which is made possible by their operations at high temperatures. In energy storage systems, the developments of the methods of recovery and restoration of heat require the knowledge of the thermal conductivity of the medium. The interest of mixtures is to have lower melting temperatures than the pure components, which increase the temperature range of their applications.

[1] Laboratoire des Interactions Moléculaires et des Hautes Pressions, CNRS, Centre Universitaire Paris-Nord, 93430 Villetaneuse, France.

0195-928X/85/0700-0315$04.50/0

840/6/4-1

As molten salts are very corrosive materials and as they also have, in general, high melting points, the measurement of their thermal conductivity is not easy. The main difficulties arise from contributions of convection and radiation to the heat transfer mechanism.

Several measurements reported in the literature have shown a large increase in the thermal conductivity of molten salts with increasing temperatures, which is not common for liquids, with the exception of water. Large discrepancies in experimental data were also observed; they are larger than the claimed respective accuracies of the data.

In this paper, we present new measurements of the thermal conductivity of molten salts using a steady-state method with a coaxial cylindrical cell having a small gap, to minimize the radiation correction.

2. EXPERIMENTAL METHOD

The cell, made of silver, is shown in Fig. 1. The centering of the internal cylinder (I) is realized by six alumina pins set in the internal cyclinder. The surfaces limiting the sample were carefully polished. We verified the nonmodification of the surfaces after the run of measurements. The emissivity coefficient was as low as possible ($\varepsilon = 0.02$). The internal cylinder is 120 mm in length and 20 mm in diameter. The external cylinder (E) is 50 mm in external diameter and 200 mm in length. The layer G between the cylinders is 0.2 mm thick. This small value was selected to minimize the exchange of heat by convection and the corrections related to the radiation–conduction coupling. A platinum sheath (0.1 mm in thickness) containing a resistor (R) is placed axially in the internal cylinder. The resistor is used to generate the temperature gradient in the layer. In opposite holes, drilled 1 mm from the external surface, two platinum sheaths are inserted which contain nisil–nicrosil thermocouples. In the external cylinder (E), two platinum sheaths are also inserted to receive thermocouples. Their ends are located at 1 mm of the external surface. Then the temperature difference between the two cylinders is measured by four thermocouples in opposition. The upper and lower closing pieces (U and L, respectively), made of silver, are maintained at a distrance of 0.2 mm from the inner cylinder. The heat power which is emited in the internal cylinder is transmitted to the external cylinder and the closing pieces. A part of this heat is also transferred by the centering pins, the thermocouples and their sheaths, and the electrical wires and their sheaths. A calibration was made to estimate these losses. A quartz container (S) (Fig. 2) filled with the salt and the cell (T) are set up in a variable-volume enclosure. This entire device is located in the axis of a vertical cylindrical

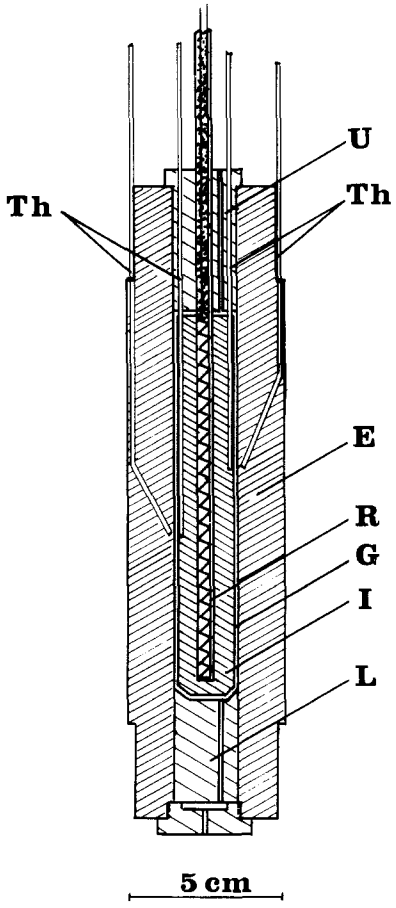

Fig. 1. Experimental cell for thermal conductivity measurements. Th, thermocouples; E, external cylinder; I, internal cylinder; R, electrical resistor; G, gap filled with the salt; U, upper closing piece; L, lower closing piece.

furnace (F). This furnace is made of copper and supplied with three heating coils. The temperature of the furnace is raised above the melting temperature of the salt under study. Vacuum is provided in the enclosure in order to degas the sample. Then the cell is immersed in the molten salt. The level of the liquid is about 2 cm above the top of the cell. When the filling is over, dry argon gas is admitted in the enclosure. By adjusting the electrical power imparted to the different coils of the furnace, longitudinal gradients

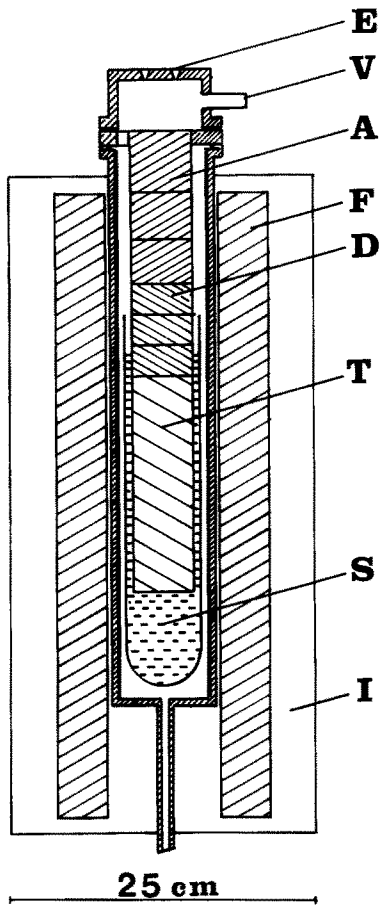

Fig. 2. Experimental setup for thermal conductivity measurements. E, electrical feedthroughs; V, vacuum pipe; A, stainless-steel disks; F, copper furnace; D, copper disks; T, thermal conductivity cell; S, molten salt container; I, insulator.

are canceled. The power emitted by the internal resistor is adjusted to set a temperature difference of the order of 1.5°C between the cylinders. This power is close to 15 W in the case of NO_3Na. When the steady state is reached, the different quantities necessary for the determination of the thermal conductivity are measured, i.e., the power dissipated in R, the temperature difference between the cylinders, and the temperature of the external cylinder taken near the fluid layer.

3. EXPERIMENTAL RESULTS

Measurements were performed on pure $NaNO_3$, KNO_3, and $NaNO_2$, the equimolar mixture KNO_3–$NaNO_3$, and HITEC. The temperature ranges which were covered in these experiments varied from the melting temperature to about 100°C above the melting temperature.

3.1. Thermal Conductivity of $NaNO_3$

The thermophysical properties of $NaNO_3$ have been extensively investigated. However, large discrepancies exist among the various data reported in the literature. Our measurements of the thermal conductivity of $NaNO_3$ are presented in Table I. In Fig. 3, our thermal conductivity data are compared with those in the literature. As can be seen, most of the measurements show an increase in the thermal conductivity with increasing temperatures. In contrast to the above, we have found that λ is almost constant.

Most of the measurements of thermal conductivity were obtained by the concentric cylinder method. Bloom et al. [1] used this type of cell, with guard rings to eliminate the heat losses at the ends. However, this method requires an accurate measurement of the axial temperature gradient. If not properly accounted for, large errors are introduced in the heat flow measurement.

The cell of White and Davis [2] has a fluid layer of 2.18 mm. Such a gap is already too large to avoid important contributions of the heat transfer by convection and radiation. The authors estimate that the main correction is related to the heat losses of the internal cylinder, which are about 20 to 33% of the total power. They also assume that the radiation correction is probably negligible, as molten salts are strong absorbers. They found that the thermal conductivity increases with the temperature following the relation

$$\lambda = 0.419 + 4.77 \times 10^{-4}\, t \qquad \text{for} \quad 340 \leqslant t \leqslant 420°\text{C} \tag{1}$$

Table I. Thermal Conductivity of $NaNO_3$

	t (°C)									
	320	320	325	341	356	362	364.5	376	393	399.7
λ ($W \cdot m^{-1} \cdot K^{-1}$)	0.510	0.514	0.510	0.516	0.512	0.514	0.511	0.516	0.512	0.506

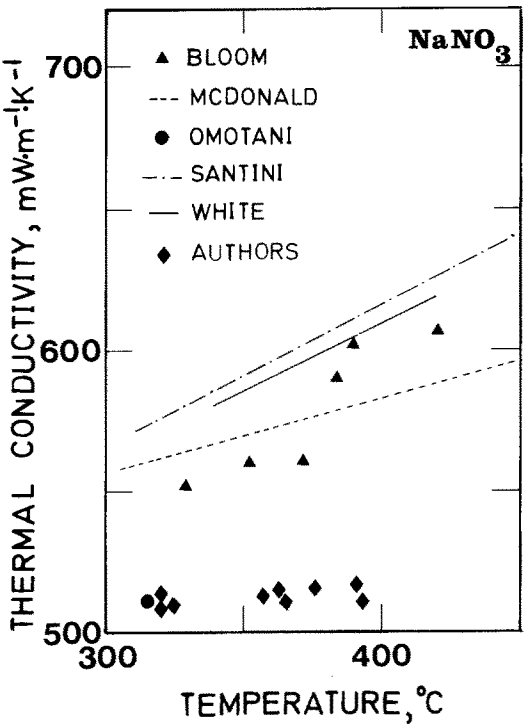

Fig. 3. Thermal conductivity of $NaNO_3$.

A smaller gap (2.5 mm) was used by McDonald and Davis [3] to measure the thermal conductivity of some alkali nitrates and their mixtures in a coaxial cylinder apparatus. They found the following variation for the thermal conductivity of $NaNO_3$:

$$\lambda = 0.4755 + 2.68 \times 10^{-4} t \qquad \text{for} \quad t < 460°C \tag{2}$$

The cell developed by Santini et al. [4] is a fluid layer enclosed between two copper disks. A vertical constant heat flow goes down through different layers: fluxmeter, fluid layer, and fluxmeter. As it is a relative technique, a calibration was made with a silicon oil having a thermal conductivity of $0.147\ W \cdot m^{-1} \cdot K^{-1}$. Their results were expressed by the relation

$$\lambda = 0.4166 + 5 \times 10^{-4} t \qquad \text{for} \quad 310 < t < 510°C \tag{3}$$

In Eqs. (1), (2), and (3), λ is in $W \cdot m^{-1} \cdot K^{-1}$ and t in °C.

These authors have stressed that with this type of arrangement, the convection was negligible. However, the large deviation with respect to our data may be due to the presence of radiation, which can explain the increase in the thermal conductivity with the temperature, or an erroneous account of heat losses through the calibration. Our own experience has shown that heat losses generally increase with the thermal conductivity of the test fluid and that a true calibration can be made only with a standard fluid having a thermal conductivity of the same order of magnitude of that of the test fluid. Moreover, the thermal conductivity of liquids is generally not known with an accuracy better than 5%.

An original method of measurement by a modified transient hot-wire method using a liquid metal in a capillary as a heat source was developed by Omotani et al. [5]. They performed measurements on pure $NaNO_3$ and three mixtures with $NaNO_3$–KNO_3 in the temperature range from 498 to 593 K. Some authors have stressed that in a transient hot-wire apparatus, the radiation correction can be neglected [6]. For $NaNO_3$, their thermal conductivity value is in perfect agreement with our data.

3.2. Thermal Conductivity of KNO_3

Our measurements of the thermal conductivity of KNO_3 are given in Table II. Our results show that this thermal conductivity is almost temperature independent. In contrast to the above, most of the previous results show an increase in λ with temperature (Fig. 4). In the literature, the following equations are given. White and Davis [2]:

$$\lambda = 0.2627 + 4.98 \times 10^{-4} t \quad \text{for} \quad 340 < t < 430°C \tag{4}$$

McDonald and Davis [3]:

$$\lambda = 0.337 + 3.641 \times 10^{-4} t \quad \text{for} \quad 330 < t < 460°C \tag{5}$$

Santini et al. [4]:

$$\lambda = 0.29 + 4.04 \times 10^{-4} t \quad \text{for} \quad 350 < t < 500°C \tag{6}$$

Table II. Thermal Conductivity of KNO_3

	t (°C)				
	343.6	356	382	408	427
λ ($W \cdot m^{-1} \cdot K^{-1}$)	0.422	0.416	0.423	0.420	0.420

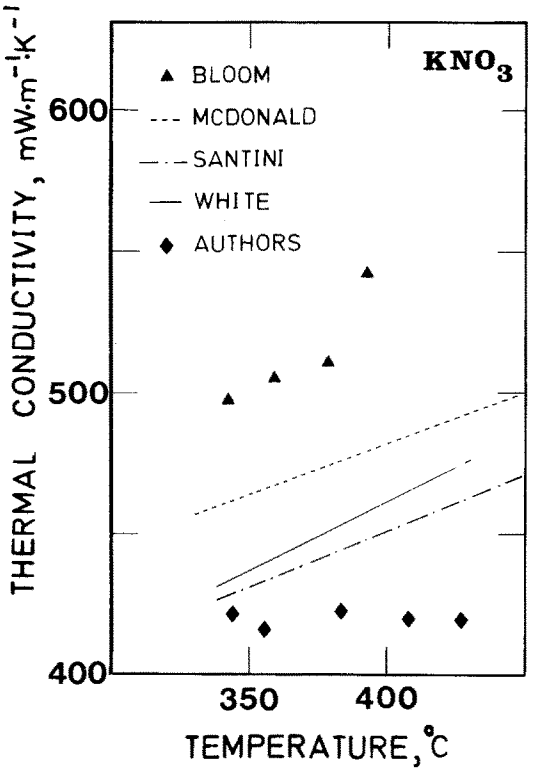

Fig. 4. Thermal conductivity of KNO_3.

3.3. Thermal Conductivity of $NaNO_2$

Our measurements of λ for $NaNO_2$ as a function of temperature are given in Table III. The temperature range is limited to avoid decomposition. There are only a few measurements of the thermal conductivity of $NaNO_2$, as shown in Fig. 5. The equation reported by Santini et al. [4] to represent the variation of thermal conductivity is

$$\lambda = 0.408 + 5.8 \times 10^{-4} t \qquad \text{for} \quad 330 < t < 490°C \tag{7}$$

3.4. Thermal Conductivity of $NaNO_2$–KNO_3 (0.5–0.5 Mole Fraction)

This equimolar molten salt mixture is known as draw salt and was proposed as a heat transfer fluid and thermal energy storage medium for various solar energy applications. In those applications the maximum operating temperature will be in the range 500–600°C. Our measurements

Table III. Thermal Conductivity of $NaNO_2$

	t (°C)	
	286	324.5
λ ($W \cdot m^{-1} \cdot K^{-1}$)	0.530	0.528

of the thermal conductivity of this salt mixture are reported in Table IV. For this mixture McDonald and Davis [3] found the following behavior for thermal conductivity:

$$\lambda = 0.439 + 2 \times 10^{-4} t \qquad \text{for} \quad t < 460°C \tag{8}$$

which leads to values about 6% higher at 251°C and 12% higher at 398°C than our data.

On the other hand, a good agreement was found with the data of Omitani et al. [5], as shown in Fig. 6.

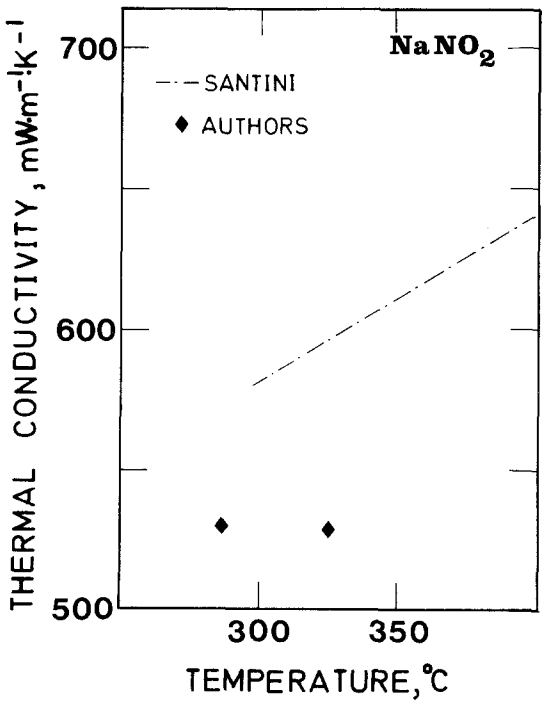

Fig. 5. Thermal conductivity of $NaNO_2$.

Table IV. Thermal Conductivity of $NaNO_3$–KNO_3 (0.5–0.5 Mole Fraction)

	t (°C)			
	251	314	365	398
λ ($W \cdot m^{-1}K^{-1}$)	0.460	0.460	0.458	0.450

It is interesting to note the influence of the composition for the mixture $NaNO_3$–KNO_3. This is shown in Fig. 7, where various thermal conductivity data reported in the literature are plotted in terms of the composition, all at 334°C. A rather good agreement was found with the data of Omotani et al. [5]. However, it seems that their extrapolated value for the thermal conductivity of KNO_3 ($\lambda = 0.39\ W \cdot m^{-1} \cdot K^{-1}$) is too low compared to our data ($0.420\ W \cdot m^{-1} \cdot K^{-1}$). The data of McDonald and Davis [3] show the same composition dependence (same slope) but are slightly higher. For all these mixtures a linear dependence of thermal conductivity with composition is expected.

3.5. Thermal Conductivity of $NaNO_3$–$NaNO_2$–KNO_3 (0.07–0.40–0.53 wt %)

This mixture is known as HTS (heat transfer salt) or HITEC. Owing to its low cost and low melting point it was frequently used as a heat trans-

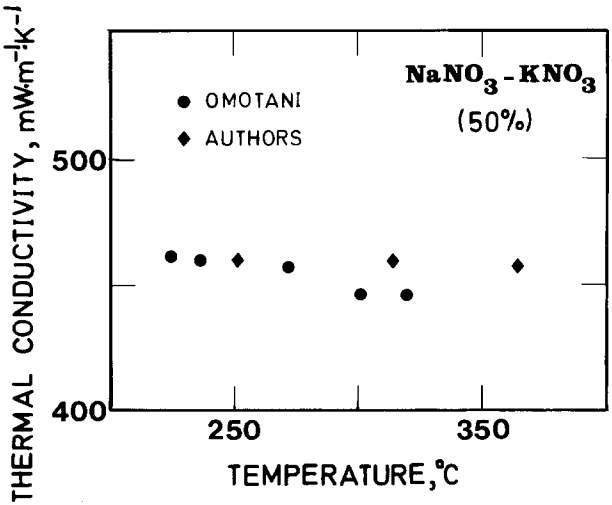

Fig. 6. Thermal conductivity of the equimolar mixture KNO_3–$NANO_3$.

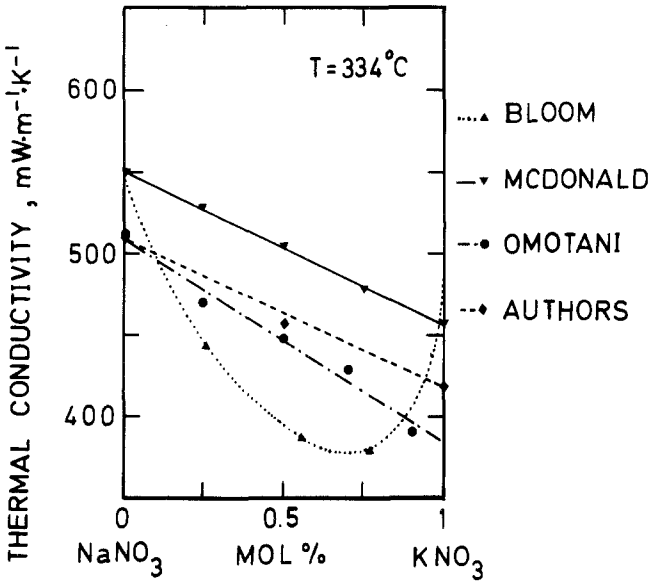

Fig. 7. Composition dependence of the thermal conductivity of $NaNO_3$–KNO_3 mixtures at 334°C.

fer fluid after the suggestion by Kirst et al. [7]. Our thermal conductivity measurements are given in Table V.

This mixture was also studied by Santini et al. [4], who reported the following equation for $170 < t < 510$°C

$$\lambda = 0.78 - 1.25 \times 10^{-3} (t + 273.15) + 1.6 \times 10^{-6} (t + 273.15)^2 \qquad (9)$$

Thus, a large increase above 300°C in the thermal conductivity of HITEC as a function of temperature was found by these authors (Fig. 8).

Table V. Thermal Conductivity of HITEC

	t (°C)			
	172.5	219	295	381
λ ($W \cdot m^{-1} \cdot K^{-1}$)	0.480	0.486	0.492	0.488

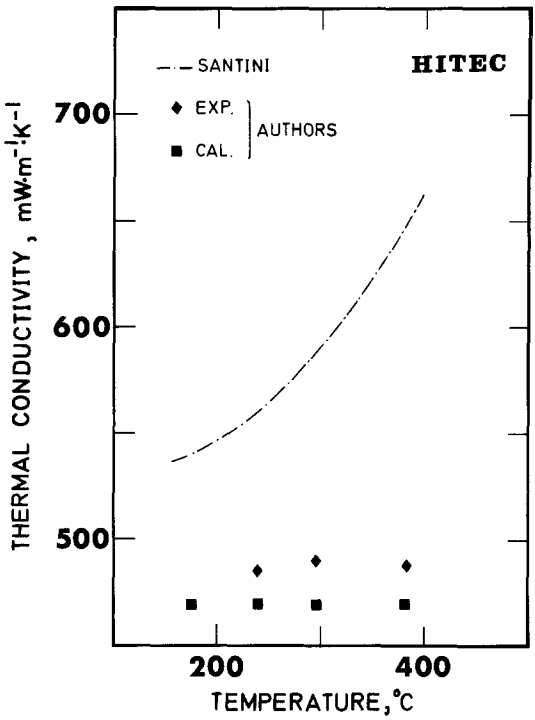

Fig. 8. Thermal conductivity of HITEC.

4. DISCUSSION

It is interesting to compare the thermal diffusion coefficients which can be calculated by the relation

$$D_T = \lambda/\rho C_p \tag{10}$$

with those reported in the literature, where ρ is the density and C_p is the specific heat at constant pressure. For the density, we use the following values in $kg \cdot m^{-3}$ as reported in Ref. 8:

$$\rho(NaNO_3) = 1927 \exp[-3.97 \times 10^{-4} (t - 310)] \tag{11}$$

$$\rho(KNO_3) = 1890 \exp[-4.19 \times 10^{-4} (t - 337)] \tag{12}$$

Several measurements of the density of $NaNO_2$ are reported in the literature. Recently, Iwadate et al. [9] gave the following temperature variation.

$$\rho(NaNO_2) = 1993 - 0.571\, t \qquad \text{for} \quad 327.15 < t < 347.35 \tag{13}$$

The densities of the equimolar mixture $NaNO_3$–KNO_3 were measured by Nissen [10] from 300 to 600°C, which may be represented by

$$\rho(NaNO_3\text{–}KNO_3) = 2090 - 0.636\,t \tag{14}$$

These values are in good agreement with the value obtained from the density of pure components with a linear mixing rule. For HITEC the values reported by Kirst et al. [7] are 1980 $kg \cdot m^{-3}$ at the melting point and 1680 $kg \cdot m^{-3}$ at 450°C. These values are also in agreement with those determined by a linear mixing rule.

The specific heat at constant pressure is generally known with an accuracy of 5–10%.

In the case of KNO_3, a value of 141.9 $J \cdot mol^{-1} \cdot K^{-1}$ is generally accepted for C_p [8]. For $NaNO_3$, a small solid–solid transition at 277°C introduced difficulties in the study of the solid–liquid transition and the slope of the curve describing the enthalpy of the liquid. We have selected the value of C_p determined by drop calorimetry in an ice calorimeter, i.e., 139.8 $J \cdot mol^{-1} \cdot K^{-1}$ [11].

The specific heat of molten $NaNO_2$ reported by Janz and Truong [12] shows a slight negative temperature dependence over the temperature range 570–670 K (119.7 $J \cdot mol^{-1} \cdot K^{-1}$ at 570 K and 118.0 $J \cdot mol^{-1} \cdot K^{-1}$ at 630 K).

For the equimolar mixture, Kamimoto [13] reported the value 136 $J \cdot mol^{-1} \cdot K^{-1}$ in the temperature range 222–450°C.

For HITEC, measurements were made by Janz and Truong [12]. They found a slight decrease in C_p as a function of the temperature, with a value of 131.5 $J \cdot mol^{-1} \cdot K^{-1}$ near the melting temperature.

With these values of density and specific heat at constant pressure, thermal diffusivities D_T for the various salts were computed. The computed values of D_T are presented in Table VI, in the liquid phase near the melting temperature of the salts.

Table VI. Thermal Diffusivity of Some Molten Salts

Salt	Melting temp. (°C)	D_T (10^{-7} $m^2 \cdot s^{-1}$)	
		Computed	Experimental
$NaNO_3$	308	1.58	1.62 [14]
KNO_3	337	1.63	1.68]14]
$NaNO_2$	281	1.63	2.15 [15]
$NaNO_3$–KNO_3	222	1.57	
HITEC	140	1.62	

The thermal diffusivity of some molten salts ($NaNO_3$ and KNO_3) was measured by Kato et al. [14] using a metallized ceramic cell. Their measured values are in good agreement with our calculated data (deviation 3%), if we take into account the accuracy associated with the specific heat measurements. On the other hand, measurements of the thermal diffusivity of $NaNO_2$ performed by Iwadate et al. [15] by a wave-front shearing interferometry give high values (+30%).

In Fig. 9, we have plotted the thermal diffusivity of some substances as a function of temperature. It can be seen that the thermal diffusivity shows small variations in the liquid phase for substances which have thermal conductivities of the same order of magnitude (0.4 to 0.7 $W \cdot m^{-1} \cdot K^{-1}$). However in the gas phase, large variations in the thermal diffusivity are expected, as shown in Fig. 10 for ammonia, where isotherms of thermal diffusivity are plotted in terms of density. In particular, the thermal diffusivity goes to zero near the critical point.

For molten salts (Fig. 9), the surprising fact is that the thermal diffusivity so calculated increases slightly with the temperature, in contrast to the measurements of Kato et al. [14], which either give constant values or indicate a decrease with the temperature. As measurements of the specific heat at constant pressure are not very accurate, we may expect that this

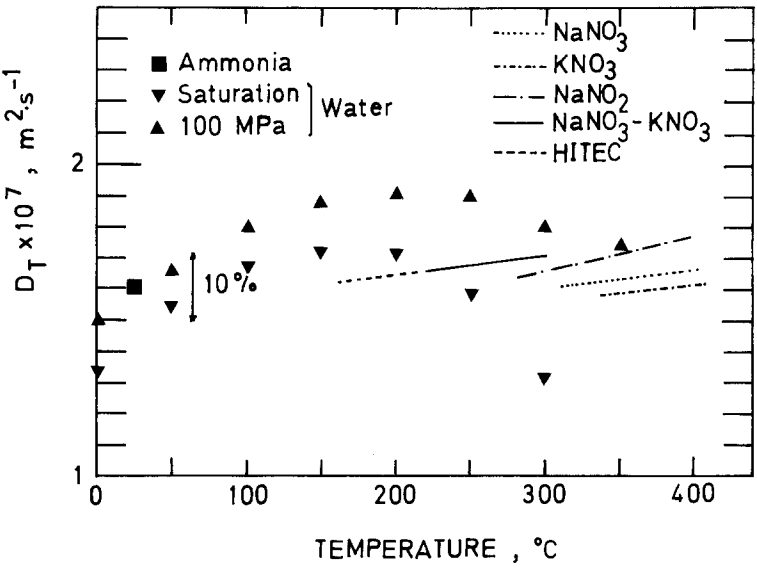

Fig. 9. Variation of the thermal diffusivity of polar and ionic compounds with temperature.

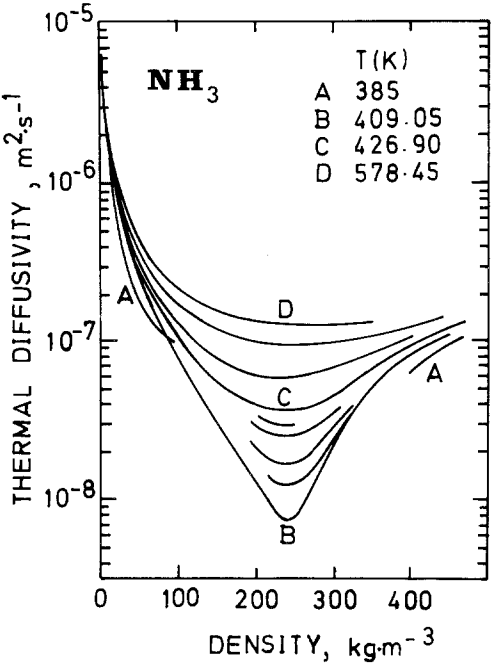

Fig. 10. Isotherms of thermal diffusivity of ammonia as a function of density.

quantity for molten salts increases slowly with the temperature, as is the case for other fluids.

Another remark is that near the melting temperature, the thermal diffusivity is almost constant ($D_T \simeq 1.62 \times 10^{-7}\ m^2 \cdot s^{-1}$) for the molten salts that we have studied. Thus, an estimation of the specific heat at constant pressure can be made with these assumptions, as reported in Table VII.

Table VII. Specific Heat at Constant Pressure of Molten Salts and Their Moxtures at Melting Temperatures

	C_P ($J \cdot mol^{-1} \cdot K^{-1}$)	
Salt	Computed	Experimental
$NaNO_3$	137	135–139.8
KNO_3	141	141.9
$NaNO_2$	122	117–121
$NaNO_3$–KNO_3(50%)	136	136–156
HITEC	132	131–153

5. CONCLUSION

Several measurements of the thermal conductivity of molten salts and their mixtures are reported. The accuracy of the measurements was estimated to be better than $\pm 4\%$. Generally we found lower values than those measured up to now, with the exception of the data of Omotani et al. [5]. In the temperature range of this investigation, the thermal conductivity was found to be temperature independent. The thermal conductivity of a mixture can be calculated by a simple linear mixing rule, as sown for HITEC (Fig. 8). The thermal diffusivity is almost constant ($D_T = 1.62 \times 10^{-7}\ m^2 \cdot s^{-1}$) for the systems that we have studied, and this value can be used to estimate the specific heat at constant pressure of binary mixtures, $NaNO_3$–KNO_3, $NaNO_2$–KNO_3, and $NaNO_3$–$NaNO_2$, or ternary mixtures, $NaNO_3$–KNO_3–$NaNO_2$.

ACKNOWLEDGMENT

We are grateful to Mr. H. Watanabe, National Research Laboratory of Metrology (Japan), for his great help in performing the experiments.

REFERENCES

1. H. Bloom, A. Doroskowski, and S. B. Tricklebank, *Ast. J. Chem.* **18**:1171 (1965).
2. L. R. White and H. T. Davis, *J. Chem. Phys.* **47**:5433 (1967).
3. J. McDonald and H. T. Davis, *J. Phys. Chem.* **74**:725 (1970).
4. R. Santini, L. Tadrist, J. Pantaloni, and P. Cerisier, *Int. J. Heat Mass Transfer* **27**:623 (1984).
5. T. Omotani, Y. Nagasaka, and A. Nagashima, *Int. J. Thermophys.* **3**:17 (1982).
6. C. A. Nieto de Castro, S. F. Y. Li, G.C. Maitland, and W. A. Wakeham, *Int. J. Thermophys.* **4**:311 (1983).
7. W. E. Kirst, W. N. Nagle, and J. B. Castner, *AICHE* **5**:371 (1940)
8. D. Sirousse-Zia, L. Denielou, J. P. Petitet, and C. Tequi, *J. Phys. Lett.* **38**:L61 (1977).
9. Y. Iwadate, I. Okada, and K. Kawamura, *J. Chem. Eng. Data* **27**:288 (1982).
10. D. A. Nissen, *J. Chem. Eng. Data* **27**:269 (1982).
11. L. Denielou, J. P. Petitet, C. Tequi, M. Fraiha, and D. Sirousse-Zia, in press.
12. G. J. Janz and G. N. Truong, *J. Chem. Eng. Data* **28**:201 (1983).
13. M. Kamimoto, *Bull. Electrotech. Lab.* **46**:532 (1982) (Japanese).
14. Y. Kato, K. Furukawa, N. Araki, and K. Kobayasi, *High Temp. High Press.* **15**:191 (1983).
15. Y. Iwadate, I. Okada, and K. Kawamura, *Chem. Soc. Jap.* **6**:969 (1982).